

# Approximate Cross-validated Mean Estimates for Bayesian Hierarchical Regression Models

Amy Zhang\*

Department of Statistics, Pennsylvania State University  
and

Le Bao

Department of Statistics, Pennsylvania State University  
and

Michael J. Daniels

Department of Statistics, University of Florida

December 22, 2024

## Abstract

We introduce a novel procedure for obtaining cross-validated predictive estimates for Bayesian hierarchical regression models (BHRMs). Bayesian hierarchical models are popular for their ability to model complex dependence structures (e.g., Gaussian processes and Gaussian Markov random fields) and provide probabilistic uncertainty estimates, but can be computationally expensive to run. Cross-validation (CV) is therefore not a common practice to evaluate the predictive performance of BHRMs. Our method circumvents the need to re-run computationally costly estimation methods for each cross-validation fold and makes CV more feasible for large BHRMs. By conditioning on the variance-covariance parameters, we shift the CV problem from probability-based sampling to a simple and familiar optimization problem. In many cases, this produces estimates which are equivalent to full CV. We provide theoretical results and demonstrate its efficacy on publicly available data and in simulations.

*Keywords:* Bayesian hierarchical regression models, Gaussian latent variable models, leave-one-out, leave-cluster-out, plug-in estimators

---

\*This work was supported by the NIH/NIAID under grant 5-R01-AI136664.

# 1 Introduction

Bayesian hierarchical models (BHM) are often used for their ability to model complex dependence structures while producing probabilistic uncertainty estimates. Except for the simplest of models, BHMs require computationally expensive methods such as Markov Chain Monte Carlo (MCMC) to obtain the posterior density. This has led to many papers which either present new methods to approximate the posterior density (e.g., Kingma and Welling, 2013; Lewis and Raftery, 1997; Rue et al., 2009) or attempt to make current methods more efficient (Bardenet et al., 2017; Korattikara et al., 2014; Quiroz et al., 2019).

The computational cost of a BHM increases by an order of magnitude when cross-validation (CV) is used, where it then becomes necessary to repeat the posterior density estimation process for each CV fold. This can be mitigated by reducing the number of folds—however, when the data are not independent of each other, random  $K$ -fold cross-validation selects models which overfit because of the high correlation between test and training data (Arlot et al., 2010; Opsomer et al., 2001). In models with complex dependency structures, it is widely preferred to use a CV scheme that could reduce this correlation, often resulting in a number of folds far beyond standard 10-fold CV.

We address the computational cost of cross-validation by introducing a novel procedure for obtaining Bayesian hierarchical model (BHM) posterior mean estimates under cross-validation. We focus on regression models as they are widely used. In general, the method also applies to models that can be written as first-stage Gaussian models with Gaussian hyperpriors, such as Gaussian processes and Gaussian Markov random fields, referred to by Vehtari et al. (2016b) as Gaussian latent variable models. In Section 2, we present our procedure, which we refer to as AXE as an abbreviation for (A)pproximate (X)cross-validation (E)stimates. The procedure can be applied to many CV schema, e.g.  $K$ -fold, leave-one-out (LOO), and leave-one-cluster-out (LCO). In Section 3, we present theoretical results establishing an upper bound on the consistency of variance parameters in BHRMs throughout CV folds for LCO CV, which also implies consistency of LOO CV. In terms of consistency, what matters is that the training data is sufficient such that the variance parameters can be well-estimated and the proof for LCO CV can be generalized to other

CV schema. In Section 4, we summarise and discuss other LCO approximation methods in the literature. In Section 5, we supply empirical results on five publicly available data sets.

## 2 Approximate cross-validation estimates using plug-in estimators

In Section 2.1, we describe notation that we use throughout the paper. We present AXE for Bayesian hierarchical linear regression models in Section 2.2, and AXE for generalized linear mixed-effects models (GLMMs) in Section 2.3.

### 2.1 Notation

Let  $Y \in \mathbb{R}^N$  denote a continuous response vector that follows

$$\begin{aligned} Y|\beta, \tau &\sim N(X_1\beta_1 + X_2\beta_2, \tau^2 I), \\ \beta_1 &\sim N(\alpha_1, C), \quad \beta_2|\Sigma \sim N(\alpha_2, \Sigma), \\ \Sigma &\sim f(\Sigma), \quad \tau \sim f(\tau), \end{aligned} \tag{1}$$

where  $X := \begin{bmatrix} X_1 & X_2 \end{bmatrix} \in \mathbb{R}^{N \times P}$  is the design matrix,  $\beta_1 \in \mathbb{R}^{P_1}$ ,  $\beta_2 \in \mathbb{R}^{P_2}$  s.t.  $\beta := \begin{bmatrix} \beta_1' & \beta_2' \end{bmatrix}' \in \mathbb{R}^P$ ,  $C \in \mathbb{R}^{P_1 \times P_1}$  is positive-definite and typically a diagonal matrix,  $\Sigma \in \mathbb{R}^{P_2 \times P_2}$  is positive-definite, and  $\tau \in \mathbb{R}_+$ . Note that  $C$  is treated as fixed, often with large variances, and thus  $\beta_1$  are referred to as the fixed effects. Random variance hyperparameters such as  $\Sigma$  reflect the dependency among the  $\beta_2$ ; the effect is to pool information among related units and shrink them towards a common mean, thus the  $\beta_2$  are referred to as random effects. We take  $\alpha_1 = \alpha_2 = 0$  throughout this paper, without loss of generality. We assume  $\mathbb{1} \in \text{span}(X_1)$ , where  $\mathbb{1}$  is the  $N$ -length vector of ones, which means that the fixed effects include a global intercept or set of intercepts which partition the data.

Posterior means  $E[\Sigma|Y]$  and  $E[\tau|Y]$  are denoted as  $\hat{\Sigma}$  and  $\hat{\tau}$ , respectively. Given a vector  $Y$  or matrix  $X$  and set of indices  $j \subset \{1, \dots, N\}$ ,  $n_j = |j|$  refers to the cardinality of set  $j$ ,  $Y_j \in \mathbb{R}^{n_j}$  refers to the vector of entries in  $Y$  indexed by  $j$ , and  $X_j \in \mathbb{R}^{n_j \times P}$  refers to

the rows of  $X$  indexed by  $j$ . For example,  $j$  may contain the indices of the test data; then  $Y_j$  is the test data response vector.  $Y_{-j} \in \mathbb{R}^{N-n_j}$  refers to the vector  $Y$  without the entries indexed by  $j$ , and likewise for  $X_{-j} \in \mathbb{R}^{N-n_j \times P}$ , the matrix without the rows indexed by  $j$ .

## 2.2 AXE for linear mixed models

When modeling data as in Equation (1), the posterior mean for  $X\beta$  conditioned on variance parameters has the form

$$E[X\beta|\Sigma, \tau^2, Y] \sim \tau^{-2} X V X' Y, \quad V = \left( \tau^{-2} X' X + \begin{bmatrix} C^{-1} & 0 \\ 0 & \Sigma^{-1} \end{bmatrix} \right)^{-1}. \quad (2)$$

Our method is based on the observation that  $\tau^{-2} X V X'$  depends only on the variance and covariance parameters  $(\tau, C, \Sigma)$  and the design matrix  $X$ . It can be shown that this matrix of weights is equivalent to the shrinkage and pooling factors of Efron and Morris (1975) for one-way models when  $\hat{\Sigma}$  and  $\hat{\tau}$  are used as plug-in estimates for Equation (2) and  $C^{-1}$  is taken as the matrix of 0s, which corresponds to the assumption that the fixed effects have infinite variance. Kass and Steffey (1989) show that, for a one-way model, the posterior mean  $E[\beta|Y] = E[\beta|Y, \hat{\tau}_{\text{EB}}, \hat{\Sigma}_{\text{EB}}](1 + \mathcal{O}(P_2^{-1}))$ , where  $\hat{\tau}_{\text{EB}}, \hat{\Sigma}_{\text{EB}}$  denote the Empirical Bayes estimates. They note that  $\hat{\Sigma}_{\text{EB}}$  in turn approximates  $\hat{\Sigma}$  with order  $\mathcal{O}(P_2^{-1})$ . Conditioning on variance parameters then produces estimates which approximate the posterior mean. The accuracy of this approximation is simple to determine by comparing the conditional expectation  $E[X\beta|\hat{\Sigma}, \hat{\tau}, Y]$  to the posterior expectation  $E[X\beta|Y]$ .

AXE extends this idea to cross-validation, using the full data posterior means of the variance and covariance parameters  $\hat{\tau}$  and  $\hat{\Sigma}$  as plug-in estimates for Equation (2) and removing the test data  $j \in \{1, \dots, N\}$  from  $X$ . When  $E[\Sigma|Y_{-j}] \approx E[\Sigma|Y]$ , this re-creates the matrix of weights for the training data and can be used to obtain approximations of the cross-validation estimates. The AXE approximation for CV mean estimate  $E[Y_j|Y_{-j}]$  is

$$\hat{Y}_j^{\text{AXE}} = E[X\beta|Y_{-j}, \hat{\Sigma}, \hat{\tau}] = \frac{1}{\hat{\tau}^2} X_j \left( \frac{1}{\hat{\tau}_{-j}^2} X_{-j}' X_{-j} + \begin{bmatrix} 0 & 0 \\ 0 & \Sigma^{-1} \end{bmatrix} \right)^{-1} X_{-j}' Y_{-j}. \quad (3)$$

This shifts the CV problem from probability-based sampling and density estimation methods to the same form as maximum likelihood methods for simple linear regression and is likewise  $\mathcal{O}(N^2P + P^3)$  in time for each CV fold. In comparison, Gibbs sampling of the same problem (when available) is  $\mathcal{O}(SN^3P + SNP^2 + SP^3)$  in time for each CV fold, where  $S$  is the number of MCMC sampling iterations.

## 2.3 AXE for GLMMs

When the first stage of a BHRM is modeled with a non-normal distribution, the normal priors on the coefficients  $\beta$  are no longer conjugate and the analytic solution from Equation (2) is not available. We can instead approximate the first stage of the GLMM using a normal distribution with equivalent moments, maintaining conjugacy and a closed-form solution for AXE. Take as example a one-way GLMM with clustered response data  $Y_j$ , where  $j$  denotes the  $j^{th}$  cluster,  $n_j$  the size of the cluster, and  $t = 1, \dots, n_j$  indexes values within the  $j^{th}$  cluster. The data  $Y_{jt}$  have some probability density function  $\pi$  and are modeled as a regression through link function  $g$  so that

$$\begin{aligned} Y_{jt}|X_j\beta &\sim \pi(g^{-1}(X_j\beta)), \\ \beta|\Sigma &\sim N(0, \Sigma), \quad \Sigma \sim f(\Sigma), \end{aligned}$$

where  $E[Y_{jt}|X_j\beta] = g^{-1}(X_j\beta)$  and  $v_j := -1/\pi''(g^{-1}(X_j\beta)) = \text{var}(Y_{jt})$ . Then taking the normal approximation with equivalent moments converges as  $n_j$  becomes large:

$$\begin{aligned} Y_{jt} &\approx N(g^{-1}(X_j\beta), v_j) \\ g(Y_{jt}) &\rightarrow N\left(X_j\beta, \frac{v_j}{g'(g^{-1}(X_j\beta))^2}\right) \quad \text{as } n_j \rightarrow \infty. \end{aligned} \tag{4}$$

Denote in Equation (4) the transformed response  $g(Y_{jt})$  as  $Y_{jt}^g$ , the variance as  $\tau_j^2$ , the diagonal matrix of  $\tau_j^2$ 's as  $P(\beta)$ , and the normal approximation as  $f_N(Y_{jt}^g|X_j\beta, P(\beta))$ . When  $\Sigma$  and  $\beta$  are unknown, we plug in the marginal posterior mean  $\hat{\Sigma} = E[\Sigma|Y]$  and

$\hat{\beta} = E[\beta|Y]$ . Then,

$$X\beta|Y^g, \hat{\Sigma}, P(\hat{\beta}) \sim N_p(m, V)$$

$$V = \left( X'P(\hat{\beta})^{-1}X + \begin{bmatrix} C^{-1} & 0 \\ 0 & \hat{\Sigma}^{-1} \end{bmatrix} \right)^{-1}$$

$$m = XVX'P(\hat{\beta})^{-1}Y^g.$$

This is also known as expectation propagation where the approximating distribution is Gaussian (Minka, 2013) and has been shown to perform well by Vehtari et al. (2016b), who evaluated both Gaussian expectation propagation and Laplace approximation. Daniels and Kass (1998) showed that Gaussian expectation propagation is a Laplace approximation—it is Laplace’s method centered at the maximizer of  $f_N(Y^g|X\hat{\beta}, \hat{P})$ , while the typical Laplace approximations centers the normal approximation at the mode of the  $f_N(Y^g|\beta, P)f(\beta|\Sigma)$ . Both have  $O(\sum_j n_j^{-1})$  error (Daniels and Kass, 1998). To confirm the normal approximation is accurate enough, it is straightforward to compare numerically  $E[X_j\beta|Y, \Sigma, P(\hat{\beta})]$  to  $E[X_j\beta|Y]$ .

### 3 AXE convergence for Bayesian hierarchical regression models

AXE can be applied to any CV design. LOO-CV and LCO-CV are both popular choices for CV design. LOO-CV is often used because it maintains as much similarity to the full data model posterior as possible, while still evaluating its ability to fit to new data. LCO-CV is commonly used in models with complex dependency structures, such as spatio-temporal models or models with repeated measures. For both methods, the number of CV folds can grow with the amount of data, which can be computationally expensive, thus they typically benefit the most from CV approximation methods. We focus on proving AXE convergence under LCO-CV, which generalizes to LOO-CV.

Researchers often choose to use a non-random, structured CV design to evaluate BHRMs. In complex models, the dependency among the data can cause  $K$ -fold CV to select models

which overfit (Arlot et al., 2010; Opsomer et al., 2001). Reducing the amount of correlation between the training and test data typically results in non-random, structured CV. LCO-CV is one example of such a CV design, where the data are partitioned based on the unique values of one or more random intercepts. This is common for mixed-effects models with repeated measures. Under LCO-CV, all repeated measures for a given unit are in the test data, which provides a more realistic estimate of a model’s predictive capability for a new unit.

Without loss of generality, we take  $\theta_j$  as corresponding to a group of random effect intercepts in  $\beta_2$ , defining  $J$  total CV folds. Each unique value of  $\theta_j$  specifies membership in a cluster. This corresponds to a mixed-effects model with repeated measures. To focus on the random effects which pertain to the CV design, we rewrite  $X_1\beta_1 + X_2\beta_2$  in Equation (1) as:

$$\mu \in \mathbb{R}^N, \theta \in \mathbb{R}^N \text{ s.t. } X_1\beta_1 + X_2\beta_2 = \mu + \theta, \quad (5)$$

where  $\mu = X\beta - \theta$  contains all other fixed and random effects which do not pertain to the CV design. The test data consist of those  $Y_j$  which are distributed as  $N(\mu_j + \theta_j, \tau^2)$ . Thus  $\theta_j$  cannot be estimated from the training data, relying instead on samples drawn from hyperparameter  $\Sigma$ .

Even if  $\theta_j$  cannot be estimated from the training data,  $J - 1$  other  $\theta$ s remain and the model retains most of the information relevant to the estimation of the variance parameters. This is the mechanism which AXE relies on: the relative stability of the estimation of variance parameters across CV folds, which is formally stated in Theorem 1.

**Theorem 3.1.** *Let response vector  $Y \in \mathbb{R}^N$  of a hierarchical linear regression follow a normal distribution as in Equation (1), where  $\mathbf{1} \in \text{span}(X)$ , and prior densities  $f(\Sigma)$  and  $f(\tau)$  are  $\mathcal{O}(1)$ .  $X\beta = \mu + \theta$  as in Equation (5), where  $\theta$  has  $J$  unique values and  $\theta_1, \dots, \theta_J$ , and  $s_j$  denotes the set of indices such that  $\theta_{s_j} = \theta_j \mathbf{1}$ , and  $X_j$  is made up of identical rows.  $V$  is defined as in Equation (2). Then  $|\arg\max_{\Sigma, \tau} f(\Sigma, \tau | Y_{-\theta_j}) - \arg\max_{\Sigma, \tau} f(\Sigma, \tau | Y)| \rightarrow 0$  as  $J \rightarrow \infty$ .*

For proof, see Appendix B, provided as supplementary material.

*Remark 1.* We allow for the prior distributions of  $\tau^2$  and  $\Sigma$  to be any density, as long as the resulting posterior is proper. One of the appeals of Bayesian modeling is its flexibility and for regression models this often occurs through placing different priors on  $\Sigma$ , e.g. variable selection or Bayesian penalized splines. There is also a growing preference for half-t priors over the traditional inverse-gamma (Gelman et al., 2006; Polson et al., 2012). These considerations make it pragmatic to provide proofs for unspecified  $f(\tau^2)$  and  $f(\Sigma)$ , as non-conjugate priors are a significant portion of Bayesian modeling.

*Remark 2.*  $\mathbb{1} \in \text{span}(X_1)$  is a restriction fulfilled by having a grand mean term or set of fixed effect intercepts which partition the data.

## 4 Existing LCO methods

We compare AXE to two types of LCO methods: ghosting (GHOST) (Marshall and Spiegelhalter, 2003) and integrated importance sampling (iIS) (Li et al., 2016; Vanhatalo et al., 2013; Vehtari et al., 2016b). We use the notation for LCO-CV in Equation (5), where cluster-specific random effects are denoted as  $\theta_j$  and the remainder of the mean estimate is referred to as  $\mu$ . Under LCO-CV,  $\theta_j$  is no longer informed by any data, but by  $\theta_{-j}, \Sigma | Y_{-j}$ . All three categories of LCO methods address the discrepancy between full-data and training data posterior samples of  $\theta_j$  in different ways.

Ghosting draws  $\tilde{\theta}_j^{(s)}$  from  $f(\theta_j | \theta_{-j}^{(s)}, \Sigma^{(s)}, Y)$  for each posterior sample  $s$ . The  $S$  total “ghost” samples are then used as an approximation of  $f(\theta_j | Y_{-j})$ . If  $\theta_j$  and  $\theta_i$ ,  $i \neq j$ , are independent given  $\Sigma$ , then the ghost samples  $\tilde{\theta}_j^{(s)}$  are simply drawn from  $\theta_j | \Sigma^{(s)}$ . This mimics the effect of treating the held-out test data  $Y_j$  as a new, unknown cluster. Using the full-data posterior densities for  $\mu$  and  $\Sigma$  directly does introduce bias; if  $\theta_j \sim N(0, \sigma^2)$ , for some parameter  $\sigma^2$ , then the ghosting estimate for  $E[Y_j | Y_{-j}]$  is  $E[\mu | Y]$  rather than  $E[\mu | Y_{-j}]$ .

iIS methods integrate out the cluster-specific effects  $\theta_j$  using the importance sampling weights of Gelfand et al. (1992). Importance sampling (IS) approximates the target training-data posterior density  $\beta, \tau$  by re-weighting full-data posterior samples. The



weights  $w_j^{(s)}$  for a sample  $s$  are proportional to a ratio of the two densities,

$$w_j^{(s)} = \frac{1}{f(Y_j|\tau^{(s)}, \beta^{(s)})} = \frac{1}{f(Y_j|\tau^{(s)}, \beta^{(s)}, Y_{-j})} \propto \frac{f(\beta^{(s)}, \tau^{(s)}|Y_{-j})}{f(\beta^{(s)}, \tau^{(s)}|Y)}.$$

The equality follows from the independence of the  $Y_j$ 's given  $\beta, \tau$ . Mean estimates are obtained by averaging over the posterior samples, weighted by  $w_j^{(s)}$ :

$$\hat{Y}_j^{IS} = C \sum_{s=1}^S X \beta^{(s)} w_j^{(s)}.$$

$C = \frac{1}{\sum_{s=1}^S w_j^{(s)}}$  is a correction for knowing the ratio only up to a constant (Gelfand, 1996).

We differentiate between two iIS methods in the literature: iIS which integrates out only  $\theta_j$  (Li et al., 2016; Vanhatalo et al., 2013) and iIS which integrates over all mean parameters  $\mu$  and  $\theta$  (Vehtari et al., 2016b). We refer to the former as iIS-C, for ‘‘cluster-specific only’’ integration and the latter as iIS-A for integrating over ‘‘all coefficients’’. The weights and estimates under iIS-C and iIS-A are

$$\begin{aligned} \text{iIS-C: } w_j^{(s)} &= \frac{1}{f(Y_j|\theta_{-j}, \tau^{(s)}, \mu^{(s)}, \Sigma^{(s)})}, & \hat{Y}_j^{\text{iIS-C}} &= \frac{\sum_{s=1}^S w_j^{(s)} \tilde{Y}_j|\theta_{-j}^{(s)}, \tau^{(s)}, \Sigma^{(s)}, \mu^{(s)}}{\sum_{s=1}^S w_j^{(s)}} \\ \text{iIS-A: } w_j^{(s)} &= \frac{1}{f(Y_j|\tau^{(s)}, \Sigma^{(s)}, Y_{-j})}, & \hat{Y}_j^{\text{iIS-A}} &= \frac{\sum_{s=1}^S w_j^{(s)} \tilde{Y}_j|\tau^{(s)}, \Sigma^{(s)}, Y_{-j}}{\sum_{s=1}^S w_j^{(s)}}, \end{aligned} \quad (6)$$

where  $\tilde{Y}_j$  represents a draw from the corresponding distribution.

Both IS and iIS methods are asymptotically unbiased for LCO CV, but in practice, IS tends to perform worse (Li et al., 2016; Merkle et al., 2019). Li et al. (2016) note that the posterior is a biased approximation of the target density  $f(\mu, \theta, \tau|Y_{-j})$ . The larger the difference between the two densities, the larger the variance of importance sampling weights and estimates (Owen, 2013). In extreme cases, large importance sampling weights on only a few points may dominate the estimate, leading to low effective sample size and an unreliable estimate.

iIS can still have high variance. The more test data is removed, the heavier the tail for  $f(\Sigma, \tau|Y_{-j})$  in comparison to  $f(\Sigma, \tau|Y)$ , and the higher the variance of the importance weights. Conversely, ghosting produces biased mean estimates, but may have smaller variance than importance sampling. When  $E[\theta_j|\theta_{-j}, \Sigma] = 0$  and  $E[\mu|Y]$  is similar to  $E[\mu|Y_{-j}]$ ,

ghosting performs well at approximating LCO-CV mean estimates regardless of the amount of test data,  $n_j$ .

In the GLMM case, analytical forms for the importance weights are no longer available. We use the normal approximation in Equation (4) to obtain approximate log-likelihood values. For iIS-C, we additionally used Monte Carlo simulation to obtain the log-likelihood values by drawing 200 samples from  $\theta_j|\theta_{-j}, \Sigma$  and averaging the likelihood of  $f(Y_j|\theta_j, \tau)$ . We found little difference in the results, confirming the accuracy of expectation propagation as noted by Vehtari et al. (2016b).

We use Pareto-smoothed importance sampling (PSIS, Gelman et al. (2014)) to stabilize the importance weights and ensure finite variance for both iIS methods. Under PSIS, the 20% largest importance weights are fit to a generalized Pareto distribution for  $M$  of the  $S$  total posterior draws, and the  $M$  largest weights are replaced by order statistics from the fitted Pareto. We supply the log-ratios  $\log w_j^{(s)}$  from Equation (6) to their R package function `loo::loo` to obtain Pareto-smoothed importance sampling estimates. In general, we found that Pareto-smoothed iIS performed similarly to or improved upon iIS without smoothing.

Table 1 summarizes the differences in assumptions among the LCO methods for approximating mean estimates. While AXE relies only on the expected values being similar, other LCO methods rely on the densities being the same or similar. Note that GHOST appears to have the strongest assumptions, but if  $E[\theta_j|\theta_{-j}, \Sigma] = 0$ , the sole assumption it relies on is that  $E[\mu|Y] = E[\mu|Y_{-j}]$ . However, both AXE and iIS are unbiased, while GHOST is not.

[Table 1 about here.]

Table 1 also includes each method’s computational complexity, with derivations in Appendix A. Note that all methods except AXE require separate calculations for all  $S$  MC samples, thus AXE is often the fastest LCO method. Manual cross-validation (MCV), when using Gibbs sampling of the same problem (if available), is the most expensive with complexity  $\mathcal{O}(S(N^3P + NP^2 + P^3))$ . However, in our example data sets and models, iIS-A was often the method which took the longest to run. Many of the models in Section 5

are fit using STAN, which uses Hamiltonian Monte-Carlo (Carpenter et al., 2017; Girolami and Calderhead, 2011), where instead of the proposal distribution being a Gaussian random walk, proposal samples are generated along the gradient of the joint density. This allows for more efficient sampling and much shorter run times. iIS-C and GHOST can also be computationally expensive, typically due to inversion of  $\Sigma$  that is necessary to obtain  $E[\theta_j|\theta_{-j}, \Sigma]$  which contributes the  $\mathcal{O}(P^3)$  term. This cost can be reduced greatly if this expectation is  $E[\theta_j|\theta_{-j}, \Sigma] = 0$  and  $\Sigma = \sigma^2 I$  for some hyperparameter  $\sigma$ ,  $\mathcal{O}(SNJ)$ , which is the case when the  $\theta_j$ ,  $j = 1, \dots, J$ , are independent and identically distributed. This brings both methods closer to AXE in terms of computing cost; however, as we show in Section 6, AXE is more consistent and can be more accurate.

## 5 Example data sets and models

We use publicly available data to compare AXE and the LCO methods described in Section 4 to manual cross-validation (MCV). This section describes each of the data sets and models in detail, with all results compiled and described together in Section 6.

### 5.1 Eight schools

The eight schools data comes from a meta-analysis conducted by Rubin (1981) on the effects of coaching on verbal SAT scores and appears frequently in the literature. The data consist of means and standard errors of treatment effects from each of the eight schools and are modeled as a one-way mixed effects model where  $j$  indicates one school,  $y_j$  is the school’s mean estimate, and  $t_j$  is the school’s standard error:

$$y_j \sim N(\mu + \theta_j, t_j^2), \quad \theta_j \sim N(0, \sigma^2), f(\mu) \propto 1, f(\sigma) \propto 1$$

where  $\mu$  and  $\sigma$  are scalar values with improper uniform priors. In this one-way model,  $\mu$  corresponds to  $X_1\beta_1$  where  $X_1$  is a vector of 1’s, while  $\theta_j$  corresponds to  $X_2\beta_2$ .

We re-create a scenario derived from Vehtari et al. (2016a), where the eight  $y_j$  are multiplied by a data scaling factor  $\alpha$ —since  $t_j$  are fixed, this has the effect of increasing

the variance  $\Sigma$  and decreasing the amount of data pooling. The model then becomes:

$$\alpha y_j \sim N(\alpha\mu + \alpha\theta_j, t_j^2), \quad \alpha\theta_j \sim N(0, \alpha^2\Sigma), f(\mu) \propto 1, f(\alpha\Sigma) \propto 1.$$

For each scaling factor  $\alpha \in \{0.1, 0.2, \dots, 3.9, 4.0\}$ , cross-validation is conducted by withholding each of the  $y_j$  in turn. The CV design is then both LCO-CV and LOO-CV because we observe one mean estimate per school.

## 5.2 Radon

The Radon data measures the log radon level of 919 houses in Minnesota and contains data on location (`county`), the level of uranium in the county (`log uranium`), and whether the house contains a basement (`basement`). It is included as part of the `rstanarm` package (Gabry and Goodrich, 2016) via Gelman and Hill (2007).

We examine three models where all three define response vector  $Y$  as the `log radon` level of the house and the `county` covariate as a random effect with  $\text{county} \sim N(0, \Sigma)$ .

$$\text{Model 1: } Y \sim N(\beta_0 + \text{county}, \tau^2),$$

$$\text{Model 2: } Y \sim N(\text{basement} + \text{county}, \tau^2),$$

$$\text{Model 3: } Y \sim N(\text{basement} + \log \text{uranium} + \text{county}, \tau^2).$$

Models were fit using the `rstanarm` package (Gabry and Goodrich (2016)), using the default priors for `stan_lmer`. Cross-validation was performed over counties, with each loop removing all houses within one county as test data. Then using the notation from Equation (5),  $\theta$  corresponds to the `county` random effect, which are also  $X_2\beta_2$ , and  $\mu$  corresponds to  $X_1\beta_1$ , which correspond to  $\beta_0$  for Model 1, `basement` for Model 2, and `basement + log uranium` for Model 3. There are 85 counties in the data with a median of 5 houses per county. Two of the counties contain data on over 100 houses, each making up over 11% of the data.

## 5.3 Radon subsets

The Radon subsets data is a set of simulations where the test data are fixed as the 23 samples from the county of Olmsted and the training data are a randomly selected subset

of counties such that the total number of counties  $J$  is  $\{3, 4, 6, 9, 12\}$  (including Olmsted) and the training data size is approximately  $\{77, 58, 46, 38, 32\}$ , which corresponds to approximate test data proportions  $\rho = \{0.3, 0.4, 0.5, 0.6, 0.7\}$ . For all combinations of  $J$  and  $\rho$ , we derive the AXE and MCV values for at most 60 different iterations of training data (for  $J = 3$  and  $\rho = 0.3$ , there are only 35 iterations available due to the data availability), using the three models in subsection 5.2. Models were again fit using the `rstanarm` package with the default priors for `stan_lmer`.

The data imbalance among counties can lead to certain counties being over-represented across the sets of training data. To mitigate this, each training data set is restricted to have a unique combination of county sizes. The combinations are such that they are within 10% of the target training data size  $\phi := 23(1 - \rho)$ , meaning that  $n_{-i}$  is within  $\phi \pm 0.1\phi$ . The sample is inversely weighted by how far the training data set size is from  $\phi$ . Within each of the 60 combinations, all matching counties are found and one final combination is sampled.

## 5.4 Esports players (ESP)

The Esports player data consist of counts of professional player statistics from the popular video game “League of Legends” for players in the North American League Championship Series from January 2020 - June 2020. In a game, two teams of five players compete to capture the opposing team’s base. The data include the player’s name (`player`); the player’s team name (`team`); the player’s position on the team (`position`); the name of the player’s character in-game (`champion`); log earned gold per minute (`log_egpm`, continuous); log damage per minute (`log_dpm`, continuous), and the player’s kills in the game (`Y`). There are 73 unique players, 10 unique teams, 5 unique positions, and 108 unique champions. The data are publicly available at [oracleselixir.com](https://oracleselixir.com), which also contains many other in-game statistics.

We model the number of kills a player  $p$  achieves in a game  $g$  on champion  $c$  as a Poisson GLMM. Let design matrix  $X_1$  corresponding to the fixed effects consist of a vector of 1’s, binary indicator vectors for `team`, binary indicator vectors for `position`, `log_dpm`,

and `log_egpm`, and let  $X_1(pgc)$  correspond to the row in  $X_1$  with player  $p$ , game  $g$ , and champion  $c$ :

$$Y_{pgc} \sim \text{Poisson}(\lambda_p)$$

$$\log(\lambda_{pgc}) = X_1(pgc)\beta + \theta_p + \phi_c,$$

where the  $\beta$ s are fixed effects,  $\theta_p$  corresponds to a player-specific random intercept, and  $\phi_c$  is a champion-specific random intercept which is crossed with players. Players are typically nested within `position` and `team`, although 5 players within the data set are represented with more than one team.

The model was fit in `rstanarm` using default priors for `stan_glm`. Cross-validation folds are defined by the player-specific random intercept  $\theta_p$ . Using the notation in Equation (5),  $\mu$  corresponds to  $X_1\beta + \phi_c$ . There are 73 total players with a median number of 33 games within the data is 33, a minimum of 2, and a maximum of 56. The AXE approximation is as described in Equation (4), where  $Y^g = \log(E[Y_j|Y])$  and  $P = \frac{1}{E[X\beta|Y]}$ .

## 5.5 Scottish Lip Cancer (SLC)

The Scottish Lip Cancer data consist of total observed male lip cancer counts collected over the time period 1975-1980 in  $J = 56$  districts of Scotland; the number of expected cases,  $E_j$ , calculated based on standardization of “population at risk” across different age groups; the percent of population employed in agriculture and forestry  $m_j$ ; and an adjacency matrix  $W$ , where  $W_{jj} = 0$ ,  $W_{ji} = 1$  if  $j$  and  $i$  are neighboring districts, and  $W_{ji} = 0$  otherwise. It is available through the `CARBayesST` package (Lee et al., 2018) in R.

The number of expected cases  $E_j$  is used as an offset in a Poisson GLMM of male lip cancer counts where

$$Y_j|\lambda_j, E_j \sim \text{Poisson}(\lambda_j E_j)$$

and  $\log(\lambda_j)$  contains the fixed and random effects of the GLMM. In this scenario, the fixed effects consist of a grand mean intercept and term linear in  $m_j$ . The random effects consist of district-level random intercepts, which are modeled such that each  $\theta_j$  is dependent on

the values of its neighbors:

$$\theta_j | \theta_{-j} \sim N(\alpha \sum_{i=1}^n W_{ij} \theta_i, \sigma^2), \quad \alpha \in [0, 1]$$

$$\log(\lambda_j) = \beta_0 + \beta m_j + \theta_j.$$

The value of  $\alpha$  controls the spatial dependence among neighboring districts, where 0 indicates no spatial dependence. The joint distribution of the  $\theta_j$  simplifies to:

$$\theta_j \sim N(0, \sigma^2(\text{diag}(W\mathbf{1}) - \alpha W)^{-1}).$$

The covariance of the  $\theta_j$  is a simplified version of what is called a proper conditional auto-regression (CAR).

The cross-validation folds are defined by the districts, thus for this example, LCO-CV is equivalent to LOO-CV.  $\theta_j$  here corresponds to  $\theta_j$  using the notation of Equation (5) and  $\mu_j$  corresponds to  $\beta_0 + \beta_j$ . The AXE approximation is as described in the normal approximation of Equation (4), where  $Y^g = \log(E[\lambda_j|Y])$ , to account for the additional offset term which is not modeled by the GLMM.

## 5.6 Scottish respiratory disease (SRD)

The Scottish respiratory disease data consist of annual observed respiratory-related hospital admissions in the  $J = 271$  Intermediate Geographies (IG) of the Greater Glasgow and Clyde health board from 2007 - 2011; the yearly average modelled concentrations of particulate matter less than 10 microns ( $\text{PM}_{10}$ ); the average property price in hundreds of thousands of pounds (**Property**); the proportion of the working age population who receive an unemployment benefit called the Job Seekers Allowance (**JSA**); the expected number of hospital admissions,  $E_{tj}$ , which is modeled as an offset-term; and the adjacency matrix  $W$ , where  $W_{jj} = 0$ ,  $W_{ji} = 1$  if  $j$  and  $i$  are neighboring districts, and  $W_{ji} = 0$  otherwise. It is available through the **CARBayesST** package in R.

We use the spatio-temporal auto-regressive model in Rushworth et al. (2014), where

observed hospital admissions for a year  $t$  and IG  $j$  are modelled as a Poisson GLMM:

$$Y_{tj} = \text{Poisson}(\lambda_{tj}E_{tj})$$

$$\log(\lambda_{tj}) = x'_{tj}\beta + s_{tj}$$

and  $x_{tj}$  is a vector containing **PM<sub>10</sub>**, **Property**, and **JSA** values for that year  $t$  and IG  $j$ . Within each year, spatial dependence among the corresponding vector of random effects  $s_t = (s_{t1}, \dots, s_{tJ})'$  is modeled with covariance matrix  $\sigma^2 Q(\alpha, W)^{-1}$ , where

$$Q(\alpha, W)^{-1} = \alpha(\text{diag}(W\mathbb{1}) - W) + (1 - \alpha)I_J, \quad \alpha \in [0, 1),$$

which induces spatial auto-correlation and is a special case of a CAR model. Temporal auto-correlation is introduced among the  $s_t$  by the conditional density of  $s_t|s_{t-1}$ :

$$s_t|s_{t-1} \sim N(\rho s_{t-1}, \sigma^2 Q(\alpha, W)^{-1}), j \in \{2, \dots, T\}.$$

The model is fit using the `CAR.ar()` function in `CARBayesST`, with the default priors.

Cross-validation is conducted along the  $J = 271$  IGs. To use the AXE approximation, we derive the joint density of  $s = (s'_1, \dots, s'_T)'$ :

$$s \sim N(0, \sigma^2[(I - \rho H)\text{blockdiag}(Q(\alpha, W))(I - \rho H)]^{-1})$$

$$H = \begin{bmatrix} 0_J & 0_{JT-J} \\ I_{JT-J} & 0_J \end{bmatrix},$$

where  $I \in \mathbb{R}^{JT \times JT}$  is the identity matrix and  $H \in \mathbb{R}^{JT \times JT}$  accounts for the temporal auto-correlation. From here, the AXE procedure is as described in the normal approximation of Equation (4), where  $Y^g = \log(E[\lambda_j|Y])$ , to account for the additional offset term which is not modeled by the GLMM. To save computation time and avoid inverting  $V_{-j} \in \mathbb{R}^{JT \times JT}$  for each cross-validation fold, we numerically solve for  $V$  given the full data and use the Sherman-Morrison matrix equations to obtain  $V_{-j}$ :

$$V_{-j} = (V^{-1} - X'_j P_j^{-1} X_j)^{-1}$$

$$= V + V X'_j (P_j - X_j V X'_j)^{-1} X_j V.$$



## 6 Results

Table 2 is a high-level summary of the differences between the example data sets and their models. The first three examples are linear mixed models (LMMs) and use AXE directly; the last three are generalized linear mixed models (GLMMs) and use instead a normal approximation of the response. The first four examples include models where  $\Sigma$  is a diagonal matrix, while the last two examples have CAR structure on the covariance of the random effects.

[Table 2 about here.]

Model estimates are often evaluated using cross-validated root mean square error (RMSE), where the error is the difference between  $E[Y_j|Y_{-j}]$  and  $Y_j$ . To compare how different RMSE is when using an LCO approximation method, we take the log ratio of approximate RMSE to ground-truth MCV RMSE. We calculate the log ratio separately within each CV fold to obtain more fine-grained comparisons of LCO results:

$$\text{LRR}_j = \log \left( \sum_{i=1}^{n_j} \frac{(\hat{Y}_{ij}^{(\text{approx. method})} - Y_{ij})^2}{(\hat{Y}_{ij}^{(\text{MCV})} - Y_{ij})^2} \right). \quad (7)$$

We compared LRRs for AXE, GHOST, iIS-C, and iIS-A across our example data sets. We also compared two variations on AXE, where instead of using the full-data posterior means  $\hat{\Sigma}$  and  $\hat{\tau}$  as plug-in estimates for Equation (3), we used the maximum a posteriori (MAP) values and the iIS estimates for  $\Sigma$  and  $\tau$ . We found that there was not much difference between the three estimates and present here the results using the full-data posterior means  $\hat{\Sigma}$  and  $\hat{\tau}$ .

Figure 1 contains boxplots of LRR for each LCO method and data set. In general, LRR for AXE approximations are consistently near 0, with lower variance than other LCO methods. Each of the other methods performs well for one or more data sets, but none perform well consistently across all data sets.

[Figure 1 about here.]

Panel A of Figure 1, with result for the Eight schools data, also includes a comparison to PSIS-LOO, for perspective. As the data scale  $\alpha$  increased, PSIS-LOO’s accuracy decreased, while the LCO approximation methods stayed consistently accurate. All LCO methods do have a few cases with high LRR for the Eight Schools data; for the LCO methods, these typically correspond to cases with low MCV RMSE and often a low data scaling factor.

Panel B of Figure 1 contains results for the full Radon data, with 919 data points and 85 clusters (counties). The Radon data is a relatively rich data set and all LCO methods perform well here, with low absolute LRR.

Panel C of Figure 1 contains results for the Radon subsets data. For Model 3, GHOST and iIS-C produce LRRs  $< -1$  which are not presented on the figure: 1.1% for GHOST and 0.3% for iIS-C. While GHOST and iIS-C have larger absolute LRR, AXE and iIS-A approximations have smaller absolute LRR. In short, this is due to differences between  $E[\mu|Y]$  and  $E[\mu|Y_{-j}]$ . In Model 2, a fixed effect intercept for `floor` is added. The majority of houses have no basement (`floor` = 0), thus there is less information for the `floor` effect, meaning  $\beta_{\text{floor}}|Y_{-j}$  is more likely to change between CV folds. Model 3 contains both the fixed `floor` effect and the continuous fixed effect for `log uranium`, which is defined at the county level only. For the full Radon data, that means there are 84 unique values of `log uranium` in the training data; for the Radon subsets data, the number of unique values ranges from 2 to 11. Thus both GHOST and iIS-C perform worse for model 3 because the support of samples for  $\mu|Y$  does not sufficiently match the support for  $\mu|Y_{-j}$ . It is interesting to note that GHOST tends to under-estimate RMSE for the Radon subsets data, while iIS-C over-estimates RMSE. As GHOST uses the full-data posteriors directly, it follows that it produces optimistic estimates. The relatively good performance of AXE and iIS-A suggests that  $f(\Sigma, \tau|Y)$  and  $f(\Sigma, \tau|Y_{-j})$  are similar enough to result in stable estimates.

All methods except iIS-A perform similarly in panels D and E of Figure 1. Diagnostics indicated that the instability of iIS-A is due to the heavier tails of the training data density  $f(\Sigma|Y_{-j})$  that lead to a large variance of the importance weights. iIS-C is not as impacted because it includes information from  $\mu|Y$ , which in this scenario produced more stable

estimates. The relatively good performance of AXE and GHOST in panel D also suggests that posterior expectations for  $\mu$  and  $\Sigma$  were relatively stable across CV folds. In panel E, the variance of LRRs for each method is larger than preceding panels (see Table 4, in Appendix C). This suggests that  $E[\Sigma, \tau|Y]$  is more different from  $E[\Sigma, \tau|Y_{-j}]$  for the SLC data than the other examples. Note that if the expectations are different, then the densities are naturally also quite different, thus both GHOST and iIS-C also do not perform as well. Panel E also included a comparison to PSIS-LOO, as LCO-CV is equivalent to LOO-CV for this example. PSIS-LOO is naturally the worst performing method, as it was for the Eight schools data set.

In the final panel for Figure 1, LRRs for iIS-A are omitted due to the amount of time running iIS-A would have required (see Table 3, with total computation time for all methods). Among the three remaining LCO approximation methods, GHOST performs the worst. Here, the auto-regressive model means  $E[\theta_j|\theta_{-j}, \Sigma] \neq 0$  and is a function of both  $\Sigma$  and  $\theta_{-j}$ . Thus any difference in the posterior densities  $f(\Sigma|Y)$  and  $f(\theta_{-j}|Y)$  versus their training data counterparts can increase error in the GHOST estimate. As iIS-C takes into account the difference between  $f(\Sigma|Y)$  and  $f(\Sigma|Y_{-j})$ , it is able to perform better than GHOST.

Table 3 provides total computation time on an Intel i7-8700k CPU with 40 Gb of memory. Except for the SRD data, models were fit using **STAN** or the **rstanarm** package, with 4 chains of 2000 samples and a 1000-sample burn-in, resulting in 4000 total samples. For the SRD data, the **CAR.ar()** function from the **CARBayesST** package was used, for four chains of 220,000 samples each, with a 20,000 sample burn-in and thinned to produce 4000 total posterior samples. In general, either AXE or GHOST takes the least amount of time. iIS-C is typically faster than MCV, but in some cases not by much, as with the Eight schools, Radon subsets, and SRD data.

[Table 3 about here.]

GHOST is generally quite fast, except for the SRD data. In the first four examples, the cluster-specific random effects  $\theta_j$  are independent and identically distributed, with  $\theta_j \sim N(0, \sigma^2)$  for some hyperparameter  $\sigma$ , thus the ghosting estimate consists of simple

draws from  $N(0, \sigma^{2(s)})$ . In both the SLC and SRD examples, the ghosting samples were drawn from the conditional multivariate normal density  $\theta_j | \theta_{-j}, \Sigma$ . An analytical solution to the conditional variance of  $\theta_j | \theta_{-j}, \Sigma$  was available for the SLC data because the LCO-CV scheme was equivalent to LOO-CV in this scenario and was used to keep computation time low. In the SRD data, it was necessary to solve for  $\Sigma^{(s)}$  by inverting the precision matrix first, which is computationally expensive.

To date iIS-A has been used only in the LOO-CV case with normal approximations, either via expectation propagation or Laplace approximations (Vanhatalo et al., 2013; Vehtari et al., 2016b). In many of our examples, iIS-A takes longer than MCV. The two cases where significant computational gains were observed were the Eight schools and SLC data sets. In those cases, where LCO-CV was also equivalent to LOO-CV and thus we were able to leverage analytical formulae for the conditional multivariate normal, particularly the Sherman-Morrison formula, attaining significant computational gains.

Figure 2A contains scatter plots of the AXE approximation for each data point  $Y_{ji}$  against actual MCV values for all examples. The vast majority of points lie on or near the 45-degree line. In many cases the AXE approximation is point-by-point equivalent to MCV estimates. This is in contrast to the scatter plots in Figure 2B, which contain AXE approximations as well as GHOST and iIS-C, both of which performed relatively well, based on Figure 1. When looking at each point individually, iIS-C has much higher variance than AXE for the Radon subsets and ESP data sets, with approximations that lie farther from the 45-degree line. GHOST has higher variance in the Eight schools, Radon subsets, and SRD data sets. All three methods perform similarly in the SLC and Radon data sets.

[Figure 2 about here.]

Some of the largest deviations from the 45 degree line are in the Radon subsets data. One would expect most LCO methods to have difficulty in approximating data with only 3 or 4 clusters, but in these cases, MCV is often straightforward to implement, and an LCO approximation method like AXE is not necessary. This example was created more as a case study to examine the behavior of AXE under a varying number of clusters and proportion

of test data. In general, we found that the accuracy of AXE was not particularly impacted as the proportion of test data increased, but it improved greatly as the number of clusters increased. This is intuitive, as a larger number of random cluster-specific intercepts means  $\Sigma$  is better-estimated and  $E[\Sigma|Y_{-j}]$  is more stable across CV folds.

## 7 Discussion

AXE is a fast and stable approximation method for obtaining cross-validated mean estimates. In our examples using publicly available data, AXE consistently performed as well or better than more computationally expensive LCO methods. This is somewhat intuitive—any large change in the estimation of  $E[\Sigma, \tau|Y_{-j}]$  across CV folds also implies a large change in  $f(\Sigma, \tau|Y_{-j})$  across CV folds, and lower accuracy for all LCO methods. However, a large change in the densities does not necessarily imply a substantial change in the variance components’ expectation across CV folds. The LCO methods we compared AXE to consisted of ghosting and integrated importance sampling. There is also a third category of LCO methods, which have been called integrated or marginal information criteria (iIC) in the literature, the most notable method of which is the integrated Watanabe-Akaike Information Criterion (Li et al., 2016; Merkle et al., 2019). iIC are used to approximate the expected log predictive density (ELPD),  $\sum_{j=1}^J \log f(Y_j|Y_{-j})$ , and do not produce estimates for  $E[Y_j|Y_{-j}]$ . They are thus omitted from comparison.

In our own experience with AXE, we have found that the cases where AXE is inaccurate are those with severe data imbalance such that the test data are critical for the estimation of  $\Sigma$  or  $\tau$ . We suggest two diagnostics for determining whether AXE could be used with confidence if there are concerns. Both require running MCV on a randomly selected subset of CV folds, stratified by clusters. The first diagnostic examines whether the hyper parameters are estimated similarly between MCV and AXE. For test data  $Y_j$ , an entry-wise matrix norm is used:  $d_j = \|\hat{\Sigma}_{\text{MCV},j} - \hat{\Sigma}_{\text{AXE}}\|$ , where  $\hat{\Sigma}_{\text{MCV},j} = E[\Sigma|Y_{-j}]$ . A small value of  $d_j$  implies the conditional densities of  $Y_j$  using  $\hat{\Sigma}_{\text{AXE}}$  and  $\hat{\Sigma}_{\text{MCV},j}$  are similar. The second diagnostic is  $\text{LRR}_j$  for each CV fold  $j$ . If exchangeability is assumed between strata, then a small sample of  $d_j$ ’s or  $\text{LRR}_j$ ’s can provide inference for the expected accuracy of AXE.

When the variance parameters  $\Sigma$  and  $\tau$  are not well-estimated, they are less likely to be consistent across CV folds; in these cases, we expect a large standard deviation among the LRRs across CV folds due to the instability of the variance parameter posterior means. We randomly sampled and compared  $\text{LRR}_j$ 's for six CV folds for the Radon, ESP, SLC, and SRD data sets. For the SLC data, the mean LRR was 0.18 with standard deviation 1.34. The high standard deviation suggests a higher degree of instability across CV folds and that MCV is likely preferable for this case. For all other data sets, we found the mean LRR and standard deviations to be low, indicating that the variance parameters are well-estimated.

# References

- Arlot, S., Celisse, A., et al. (2010), “A survey of cross-validation procedures for model selection,” *Statistics Surveys*, 4, 40–79.
- Bardenet, R., Doucet, A., and Holmes, C. (2017), “On Markov chain Monte Carlo methods for tall data,” *The Journal of Machine Learning Research*, 18, 1515–1557.
- Carpenter, B., Gelman, A., Hoffman, M. D., Lee, D., Goodrich, B., Betancourt, M., Brubaker, M., Guo, J., Li, P., and Riddell, A. (2017), “STAN: A probabilistic programming language,” *Journal of Statistical Software*, 76.
- Daniels, M. J. and Kass, R. E. (1998), “A note on first-stage approximation in two-stage hierarchical models,” *Sankhyā: The Indian Journal of Statistics, Series B*, 19–30.
- Efron, B. and Morris, C. (1975), “Data analysis using Stein’s estimator and its generalizations,” *Journal of the American Statistical Association*, 70, 311–319.
- Gabry, J. and Goodrich, B. (2016), “rstanarm: Bayesian applied regression modeling via Stan,” *R package version*, 2.
- Gelfand, A. E. (1996), “Model determination using sampling-based methods,” *Markov Chain Monte Carlo in Practice*, 145–161.
- Gelfand, A. E., Dey, D. K., and Chang, H. (1992), “Model determination using predictive distributions with implementation via sampling-based methods,” Technical report, Stanford Univ. CA Dept. of Statistics.
- Gelman, A. and Hill, J. (2007), *Data Analysis Using Regression and Multilevel/Hierarchical Models*, volume 1, Cambridge University Press New York, NY, USA.
- Gelman, A., Hwang, J., and Vehtari, A. (2014), “Understanding predictive information criteria for Bayesian models,” *Statistics and Computing*, 24, 997–1016.
- Gelman, A. et al. (2006), “Prior distributions for variance parameters in hierarchical models (comment on article by Browne and Draper),” *Bayesian Analysis*, 1, 515–534.
- Girolami, M. and Calderhead, B. (2011), “Riemann manifold Langevin and Hamiltonian Monte Carlo methods,” *Journal of the Royal Statistical Society: Series B (Statistical Methodology)*, 73, 123–214.
- Kass, R. E. and Steffey, D. (1989), “Approximate Bayesian inference in conditionally independent hierarchical models (parametric empirical Bayes models),” *Journal of the American Statistical Association*, 84, 717–726.

- Kingma, D. P. and Welling, M. (2013), “Auto-encoding variational Bayes,” *arXiv preprint arXiv:1312.6114*.
- Korattikara, A., Chen, Y., and Welling, M. (2014), “Austerity in MCMC land: Cutting the Metropolis-Hastings budget,” in *International Conference on Machine Learning*.
- Lee, D., Rushworth, A., and Napier, G. (2018), “Spatio-temporal areal unit modelling in R with conditional autoregressive priors using the CARBayesST package,” *Journal of Statistical Software*, 84.
- Lewis, S. M. and Raftery, A. E. (1997), “Estimating Bayes factors via posterior simulation with the Laplace—Metropolis estimator,” *Journal of the American Statistical Association*, 92, 648–655.
- Li, L., Qiu, S., Zhang, B., and Feng, C. X. (2016), “Approximating cross-validators predictive evaluation in Bayesian latent variable models with integrated IS and WAIC,” *Statistics and Computing*, 26, 881–897.
- Marshall, E. and Spiegelhalter, D. (2003), “Approximate cross-validators predictive checks in disease mapping models,” *Statistics in Medicine*, 22, 1649–1660.
- Merkle, E. C., Furr, D., and Rabe-Hesketh, S. (2019), “Bayesian comparison of latent variable models: Conditional versus marginal likelihoods,” *Psychometrika*, 84, 802–829.
- Minka, T. P. (2013), “Expectation propagation for approximate Bayesian inference,” *arXiv preprint arXiv:1301.2294*.
- Opsomer, J., Wang, Y., and Yang, Y. (2001), “Nonparametric regression with correlated errors,” *Statistical Science*, 134–153.
- Owen, A. B. (2013), *Monte Carlo Theory, Methods and Examples*.
- Polson, N. G., Scott, J. G., et al. (2012), “On the half-Cauchy prior for a global scale parameter,” *Bayesian Analysis*, 7, 887–902.
- Quiroz, M., Kohn, R., Villani, M., and Tran, M.-N. (2019), “Speeding up MCMC by efficient data subsampling,” *Journal of the American Statistical Association*, 114, 831–843.
- Rubin, D. B. (1981), “Estimation in parallel randomized experiments,” *Journal of Educational Statistics*, 6, 377–401.
- Rue, H., Martino, S., and Chopin, N. (2009), “Approximate Bayesian inference for latent Gaussian models by using integrated nested Laplace approximations,” *Journal of the Royal Statistical Society: Series B (Statistical Methodology)*, 71, 319–392.



- Rushworth, A., Lee, D., and Mitchell, R. (2014), “A spatio-temporal model for estimating the long-term effects of air pollution on respiratory hospital admissions in Greater London,” *Spatial and Spatio-Temporal Epidemiology*, 10, 29–38.
- Vanhatalo, J., Riihimäki, J., Hartikainen, J., Jylänki, P., Tolvanen, V., and Vehtari, A. (2013), “GPstuff: Bayesian modeling with Gaussian processes,” *Journal of Machine Learning Research*, 14, 1175–1179.
- Vehtari, A., Gelman, A., and Gabry, J. (2016a), “Practical Bayesian model evaluation using leave-one-out cross-validation and WAIC,” *Statistics and Computing*, 5, 1413–1432.
- Vehtari, A., Mononen, T., Tolvanen, V., Sivula, T., and Winther, O. (2016b), “Bayesian leave-one-out cross-validation approximations for Gaussian latent variable models,” *The Journal of Machine Learning Research*, 17, 3581–3618.

## A Computational complexity calculations

This section contains derivations for computational complexity in Table 1. We assume without loss of generality that  $\mathcal{O}(P_2) = \mathcal{O}(P)$ . For all methods, we assume that the cost of drawing a sample from a specific density is dominated by the calculation of the density's parameters, e.g. if drawing from a multivariate normal density, we assume the calculation of the mean vector and covariance matrix dominates the computational cost.

### A.1 AXE

We re-state the AXE estimate below:

$$\hat{Y}_j^{AXE} = \frac{1}{\hat{\tau}^2} X_j \left( \frac{1}{\hat{\tau}^2} X_{-j}' X_{-j} + \begin{bmatrix} 0 & 0 \\ 0 & \Sigma^{-1} \end{bmatrix} \right)^{-1} X_{-j}' Y_{-j}. \quad (8)$$

The cost of the matrix inversion in Equation (8) is  $\mathcal{O}(P^3)$ , while the matrix multiplication is  $\mathcal{O}(NP^2)$ . Conducted over  $J$  total cross-validation loops, the computational complexity for AXE is  $\mathcal{O}(J(NP^2 + P^3))$ .

### A.2 GHOST

Without loss of generality, let  $f(\theta|\Sigma)$  be  $N(0, \Sigma)$ . Then:

$$\theta_j | \theta_{-j}, \Sigma \sim N(\Sigma_{j-j} \Sigma_{-j-j}^{-1} \theta_{-j}, \Sigma_{jj} - \Sigma_{j-j} \Sigma_{-j-j}^{-1} \Sigma_{-jj}). \quad (9)$$

As we assume the dimension of  $\theta_j$  is fixed, the cost of the matrix inversion in Equation (9) is  $\mathcal{O}(P^3)$  and the cost of the matrix multiplication is likewise  $\mathcal{O}(P^3)$ . Conducted over  $J$  total cross-validation loops for  $S$  samples, the computational complexity for GHOST is  $\mathcal{O}(SJP^3)$ .

### A.3 iIS-C

We re-state the iIS-C importance weights  $w_j^{(s)}$  and mean estimate for  $E[Y_j|Y_{-j}]$ :

$$w_j^{(s)} = \frac{1}{f(Y_j | \theta_{-j}^{(s)}, \tau^{(s)}, \mu^{(s)}, \Sigma^{(s)})}, \quad \hat{Y}_j^{\text{iIS-C}} = \frac{\sum_{s=1}^S w_j^{(s)} E[Y_j | \theta_{-j}^{(s)}, \tau^{(s)}, \Sigma^{(s)}, \mu^{(s)}]}{\sum_{s=1}^S w_j^{(s)}}. \quad (10)$$

Let  $a_j := E[\theta_j|\theta_{-j}, \Sigma]$  and  $M := \text{Cov}(\theta_j|\theta_{-j}, \Sigma)$ , corresponding to the mean and covariance, respectively, of Equation (9). Then,

$$Y_j|\theta_{-j}, \tau, \mu, \Sigma \sim N(\mu + a_j, \tau^2 I + M).$$

Note that the cost of obtaining  $a_j$  and  $M$  for all CV folds and MC samples is the same as ghosting at  $\mathcal{O}(SJP^3)$ . The cost of obtaining the likelihood in weight  $w_j^{(s)}$  for Equation (10) is an additional  $\mathcal{O}\left(S \sum_{j=1}^J n_j\right) = \mathcal{O}(SN)$  and the cost of the expectation is likewise  $\mathcal{O}(SN)$ . The total cost is then  $\mathcal{O}(SJP^3)$ , the same order as ghosting.

## A.4 iIS-A

We re-state the iIS-A importance weights  $w_j^{(s)}$  and mean estimate for  $E[Y_j|Y_{-j}]$ :

$$\text{iIS-A: } w_j^{(s)} = \frac{1}{f(Y_j|\tau^{(s)}, \Sigma^{(s)}, Y_{-j})}, \quad \hat{Y}_j^{\text{iIS-A}} = \frac{\sum_{s=1}^S w_j^{(s)} E[Y_j|\tau^{(s)}, \Sigma^{(s)}, Y_{-j}]}{\sum_{s=1}^S w_j^{(s)}}. \quad (11)$$

$$Y_j|\tau^{(s)}, \Sigma^{(s)}, Y_{-j} \quad (12)$$

Note that  $Y_j|\tau^{(s)}, \Sigma^{(s)}, Y_{-j}$  is  $N(X_j V_{-j} X_{-j}' P_{-j}^{-1} Y_{-j}, P_j + X_j V_{-j} X_j')$ . Drawing from this density is equivalent to running AXE for every MC sample  $s$  and has computational cost  $\mathcal{O}(SJ(NP^2 + P^3))$  across all CV folds and MC samples. Obtaining the likelihood in  $w_j^{(s)}$  of Equation (11) has additional computational cost  $\mathcal{O}(SJN)$ . The total computational cost is then  $\mathcal{O}(SJ(NP^2 + P^3))$ .

## A.5 MCV (Gibbs sampling)

Under the model in Equation (1) with prior densities  $\Sigma \sim IW(\nu, \Psi)$ ,  $\tau \sim \Gamma^{-1}(a, b)$ ,  $\beta_1 \sim N(0, C)$ ,  $\beta_2|\Sigma \sim N(0, \Sigma)$ , one Gibbs sampling scheme is as follows:

$$\beta^{(s)}|\Sigma^{(s-1)}, \tau^{(s-1)}, Y \sim N(\tau^{-2(s-1)} V^{(s-1)} X^T Y, V^{(s-1)}), \quad (13)$$

$$V^{(s-1)} = (\Sigma^{-1(s-1)} + \frac{1}{\tau^{2(s-1)}} X^T X)^{-1}$$

$$\Sigma^{(s)}|\beta^{(s)}, \tau^{(s-1)}, Y \sim IW(N + v, \Psi + (\beta_2^{(s)} - \mu)(\beta_2^{(s)} - \mu)^T) \quad (14)$$

$$\tau^{2(s)}|\Sigma^{(s)}, \beta^{(s)}, Y \sim \Gamma^{-1}(a + \frac{1}{2}N, b + \frac{1}{2}(Y - X\beta^{(s)})^T(Y - X\beta^{(s)})). \quad (15)$$

where  $s$  refers to the  $s$ th iteration of the Gibbs sampler,  $IW$  refers to the inverse-Wishart distribution and  $\Gamma^{-1}$  the inverse-gamma.

We assume that the cost of drawing a sample from the specified densities is dominated by the re-calculation of parameters within each iteration, for example, the cost of drawing  $\beta^{(s)}$  is dominated by the calculations of  $V^{(s-1)}$  and  $V^{(s-1)}X^TY$ .

In eq. (13), the inversion of  $V$  is  $\mathcal{O}(P^3)$ , while the multiplication of  $VX^TY$  is  $\mathcal{O}(NP^2)$ . The cost of eq. (14) is  $\mathcal{O}(P_2^2)$ . The cost of eq. (15) is  $\mathcal{O}(N^2P)$ . For each iteration of the Gibbs sampler, the computational cost is  $\mathcal{O}(P^3 + NP^2 + N^2P)$ . Then with  $M$  iterations of the Gibbs sampler, the computational complexity is  $O(MN^2P + MNP^2 + MP^3)$ .

## B Proof for Theorem 1

**Lemma B.1.** *Let response vector  $Y \in \mathbb{R}^N$  of a hierarchical linear regression follow a normal distribution as in Equation (1) and let  $s_j$  be the set of indices of  $\theta_j$  in  $\theta$  such that  $X_{s_j}$  is made up of identical rows. As shorthand  $X_{s_j}$  is referred to as  $X_j$ , and  $x'_j$  is a row in  $X_j$ .  $V$  is defined as in Equation (2). We list several facts pertaining to  $V$  and  $V_{-j}$ .*

1.  $V_{-j} = V + \frac{n_j}{\tau^2} \frac{1}{1 - \frac{n_j}{\tau^2} x'_j V x_j} V x_j x'_j V$
2.  $V \preceq V_{-j}$ , where  $V \preceq V_{-j}$  indicates that  $V_{-j} - V$  is positive semi-definite
3.  $\frac{n_j}{\tau^2} x'_j V x_j \leq 1$
4.  $x'_j V_{-j} x_j = x'_j V x_j \frac{1}{1 - \frac{n_j}{\tau^2} x'_j V x_j} \geq x'_j V x_j$
5.  $\det(V_{-j}) = \det(V) \frac{1}{1 - \frac{n_j}{\tau^2} x'_j V x_j} \geq \det(V)$
6.  $\frac{1}{\tau^4} Y'_{-j} X_{-j} V_{-j} X'_{-j} Y_{-j} = \frac{1}{\tau^4} Y' X V X' Y - \frac{n_j}{\tau^2} \bar{y}_j^2 + \frac{\bar{e}_j^2}{\tau^2 / n_j} \frac{1}{1 - \frac{n_j}{\tau^2} x'_j V x_j}$

*Proof.* 1. This follows from using the Sherman-Morrison formula on  $V_{-j} = (V^{-1} - \frac{n_j}{\tau^2} x_j x'_j)^{-1}$ .

2. Using a similar process as in 1., if we re-write  $V$  in terms of  $V_{-j}$ , we obtain  $V = V_{-j} - \frac{n_j}{\tau^2} \frac{1}{1 + \frac{n_j}{\tau^2} x'_j V_{-j} x_j} V_{-j} x_j x'_j V_{-j}$ . The difference,  $\frac{n_j}{\tau^2} \frac{1}{1 + \frac{n_j}{\tau^2} x'_j V_{-j} x_j} V_{-j} x_j x'_j V_{-j}$ , is positive semi-definite and so  $V_{-j} \succeq V$ , where  $A \succeq B$  is defined as  $A - B$  is positive semi-definite.

3. From 2., we note that  $V_{-j} \succeq V$  and from 1.,  $V_{-j} - V$  is  $\frac{n_j}{\tau^2} \frac{1}{1 - \frac{n_j}{\tau^2} x_j' V x_j} V x_j x_j' V$ .  $V$  positive-definite implies  $\frac{n_j}{\tau^2} x_j' V x_j > 0$ , then for  $V_{-j} - V$  to be positive semi-definite,  $\frac{n_j}{\tau^2} x_j' V x_j \leq 1$  must be true.

4. Using 1.,  $x_j' V_{-j} x_j = x_j' V x_j + \frac{n_j}{\tau^2} \frac{1}{1 - \frac{n_j}{\tau^2} x_j' V x_j} (x_j' V x_j)^2 = x_j' V x_j (1 - \frac{n_j}{\tau^2} x_j' V x_j)^{-1}$ . The inequality follows from 3., as  $1 - \frac{n_j}{\tau^2} x_j' V x_j \leq 1$ .

5. As the held-out data correspond to identical rows of  $X$ , we have a closed-form solution for the determinant of  $V_{-j}$  in terms of  $V$ :

$$\begin{aligned} \det(V^{-1} - \tau^{-2} X_j' X_j) &= \det(V^{-1}) \det(1 - \frac{n_j}{\tau^2} x_j' V x_j) && \text{Sylvester's det. theorem} \\ &= \det(V^{-1}) (1 - \frac{n_j}{\tau^2} x_j' V x_j) \\ \implies \det(V_{-j}) &= \det(V) \frac{1}{1 - \frac{n_j}{\tau^2} x_j' V x_j} \\ &\geq \det(V) && \text{from 3.} \end{aligned}$$

6. We first show that  $\frac{1}{\tau^2} V_{-j} X_{-j}' Y_{-j} = \frac{1}{\tau^2} V X' Y + \frac{n_j}{\tau^2} \frac{\bar{e}_j}{1 - \frac{n_j}{\tau^2} \nu_j} V x_j$ . Let  $\nu_j := x_j' V x_j$ :

$$\begin{aligned} \frac{1}{\tau^2} V_{-j} X_{-j}' Y_{-j} &= \frac{1}{\tau^2} [V + \frac{n_j}{\tau^2} \frac{1}{1 - \frac{n_j}{\tau^2} \nu_j} V x_j x_j' V] (X' Y - X_j' Y_j) && \text{from 1.} \\ &= \frac{1}{\tau^2} V X' Y + V x_j \left[ -\frac{n_j}{\tau^2} \bar{y}_j + \frac{n_j}{\tau^2} \frac{1}{1 - \frac{n_j}{\tau^2} \nu_j} \left( \bar{y}_j - \frac{n_j}{\tau^2} \nu_j \bar{y}_j \right) \right] \\ &= \frac{1}{\tau^2} V X' Y - V x_j \left[ \frac{n_j}{\tau^2} \frac{1}{1 - \frac{n_j}{\tau^2} \nu_j} \bar{y}_j - \frac{n_j}{\tau^2} \frac{1}{1 - \frac{n_j}{\tau^2} \nu_j} \bar{y}_j \right] \\ &= \frac{1}{\tau^2} V X' Y + \frac{n_j}{\tau^2} \frac{\bar{e}_j}{1 - \frac{n_j}{\tau^2} x_j' V x_j} V x_j. \end{aligned}$$

Following a similar procedure, we can re-write  $\frac{1}{\tau^4} Y_{-j}' X_{-j} V_{-j} X_{-j}' Y_{-j}$  in terms of its full-data counterpart,  $\frac{1}{\tau^4} Y' X V X' Y$ , along with an additional difference term. Let  $(\tilde{Y})_{-j}$  refer

to  $X_{-j}\tilde{\beta}$ , the conditional expected value based on the full data  $Y$ .

$$\begin{aligned}
\frac{1}{\tau^4}Y'_{-j}X_{-j}V_{-j}X'_{-j}Y_{-j} &= \frac{1}{\tau^4}Y'_{-j}X_{-j}VX'Y + \frac{n_j}{\tau^4}\frac{\bar{e}_j}{1 - \frac{n_j}{\tau^2}\nu_j}Y'_{-j}X_{-j}Vx_j \\
&= \frac{1}{\tau^2}Y'_{-j}(\tilde{Y})_{-j} + \frac{n_j}{\tau^2}\frac{\bar{e}_j}{1 - \frac{n_j}{\tau^2}\nu_j}\left(\frac{1}{\tau^2}Y'XVx_j - \frac{1}{\tau^2}Y'_jX_jVx_j\right) \\
&= \frac{1}{\tau^2}Y'_{-j}(\tilde{Y})_{-j} + \frac{n_j}{\tau^2}\frac{\bar{e}_j}{1 - \frac{n_j}{\tau^2}\nu_j}\left(\tilde{y}_j - \frac{n_j}{\tau^2}\nu_j\bar{y}_j\right) \\
&= \frac{1}{\tau^2}Y'_{-j}(\tilde{Y})_{-j} + \bar{e}_j\frac{n_j}{\tau^2}\left[\frac{1}{1 - \frac{n_j}{\tau^2}\nu_j}\left(\tilde{y}_j - \frac{n_j}{\tau^2}\nu_j\bar{y}_j\right) + \bar{y}_j - \bar{y}_j\right] \\
&= \frac{1}{\tau^2}Y'_{-j}(\tilde{Y})_{-j} + \bar{e}_j\frac{n_j}{\tau^2}\left[\bar{y}_j + \frac{\bar{e}_j}{1 - \frac{n_j}{\tau^2}\nu_j}\right] \\
&= \frac{1}{\tau^2}Y'_{-j}(\tilde{Y})_{-j} + \bar{e}_j\frac{n_j}{\tau^2}\left[\bar{y}_j + \frac{\bar{e}_j}{1 - \frac{n_j}{\tau^2}\nu_j}\right] - \frac{n_j}{\tau^2}\bar{y}_j\tilde{y}_j + \frac{n_j}{\tau^2}\bar{y}_j\tilde{y}_j \\
&= \frac{1}{\tau^4}Y'XVX'Y - \frac{n_j}{\tau^2}\bar{y}_j^2 + \frac{\bar{e}_j^2}{\tau^2/n_j}\frac{1}{1 - \frac{n_j}{\tau^2}x'_jVx_j}.
\end{aligned}$$

□

**Lemma B.2.** Let response vector  $Y \in \mathbb{R}^N$  of a hierarchical linear regression follow a normal distribution as in Equation (1) and let  $s_j$  be the set of indices of  $\theta_j$  in  $\theta$  such that  $X_{s_j}$  is made up of identical rows.  $V$  is defined as in Equation (2). The difference  $\Delta_j$  between the log densities  $\ell(\Sigma, \tau|Y_{-j})$  and  $\ell(\Sigma, \tau|Y)$  is

$$\Delta_j := C + n_j \log \tau - \frac{1}{2} \log \left(1 - \frac{n_j}{\tau^2}x'_jVx_j\right) - \frac{n_j}{\tau^2}\bar{y}_j^2 + \frac{\bar{e}_j^2}{\tau^2/n_j}\frac{1}{1 - \frac{n_j}{\tau^2}x'_jVx_j},$$

where  $C \in \mathbb{R}$  is a constant that does not involve  $\Sigma$  or  $\tau$ .

*Proof.* The log-likelihood is as follows:

$$\ell(\Sigma, \tau|Y) \propto \ell(\tau) + \ell(\Sigma) - N \log(\tau) - \frac{1}{2} \log \det(\Sigma) + \frac{1}{2} \log \det(V) + \frac{1}{2\tau^4}Y'XVX'Y.$$

Using Theorem B.1, items 5 and 6, we can directly obtain the difference between the log-likelihoods  $\ell(\Sigma, \tau|Y_{-j}) - \ell(\Sigma, \tau|Y)$  as stated. □

**Lemma B.3.** Let response vector  $Y \in \mathbb{R}^N$  of a hierarchical linear regression follow a normal distribution as in Equation (1) and let  $V$  defined as in Equation (2). Let  $B := [I_{P_2}] \in \mathbb{R}^{P_2 \times P}$ , where  $I_{P_2}$  is the  $P_2$ -dimensional identity matrix. The partial derivative  $\frac{\partial}{\partial \Sigma} a'Vc$  is  $\Sigma^{-1}BVac'VB'\Sigma^{-1}$  for vectors  $a \in \mathbb{R}^P$ ,  $c \in \mathbb{R}^P$ .

*Proof.*

$$\begin{aligned}\frac{\partial}{\partial \Sigma_{ij}} V &= -V \left( \frac{\partial}{\partial \Sigma_{ij}} V^{-1} \right) V \\ &= V B' \Sigma^{-1} \delta_i \delta_j' \Sigma^{-1} B V,\end{aligned}$$

where  $\delta_i \in \mathbb{R}^{P_2}$  is the binary vector with a 1 only at the  $i^{th}$  index. Then,

$$\begin{aligned}\frac{\partial}{\partial \Sigma_{ij}} a' V c &= \frac{\partial}{\partial \Sigma_{ij}} \text{tr}(a' V b) \\ &= \text{tr} \left( b a' \frac{\partial}{\partial \Sigma_{ij}} V \right) \\ &= \text{tr} (b a' V B' \Sigma^{-1} \delta_i \delta_j' \Sigma^{-1} B V) \\ &= \text{tr} (\delta_j' \Sigma^{-1} B V c a' V B' \Sigma^{-1} \delta_i) \\ &= \delta_j' \Sigma^{-1} B V c a' V B' \Sigma^{-1} \delta_i,\end{aligned}$$

as the trace is invariant under cyclic permutations.

Then

$$\frac{\partial}{\partial \Sigma} a' V c = \Sigma^{-1} B V a c' V B' \Sigma^{-1}.$$

□

**Theorem B.4.** *Let response vector  $Y \in \mathbb{R}^N$  of a hierarchical linear regression follow a normal distribution as in Equation (1), where  $\mathbf{1} \in \text{span}(X)$ , and prior densities  $f(\Sigma)$  and  $f(\tau)$  are  $\mathcal{O}(1)$ .  $X\beta = \mu + \theta$  as in Equation (5), where  $\theta$  has  $J$  unique values and  $\theta_1, \dots, \theta_J$ , and  $s_j$  denotes the set of indices such that  $\theta_{s_j} = \theta_j \mathbf{1}$ , and  $X_j$  is made up of identical rows.  $V$  is defined as in Equation (2). Then  $|\arg\max_{\Sigma, \tau} f(\Sigma, \tau | Y_{-\theta_j}) - \arg\max_{\Sigma, \tau} f(\Sigma, \tau | Y)| \rightarrow 0$  as  $J \rightarrow \infty$ .*

*Proof.* The log-likelihood is as follows:

$$\ell(\Sigma, \tau | Y) \propto \ell(\tau) + \ell(\Sigma) - N \log(\tau) - \frac{1}{2} \log \det(\Sigma) + \frac{1}{2} \log \det(V) + \frac{1}{2\tau^4} Y' X V X' Y.$$

We note that, other than the prior densities whose forms are unknown, the log-likelihood consists of terms with  $P_2$  or  $N$  summands. As the number of CV folds is  $J$  and  $J \leq P_2$ ,  $J \leq$

$N$ ,  $J^{-1}\ell(\Sigma, \tau, Y)$  is finite and we can say that for any  $J$ , the solution to  $J^{-1}\frac{\partial}{\partial \Sigma}\ell(\Sigma, \tau|Y) = 0$  is the same as the solution to  $\frac{\partial}{\partial \Sigma}\ell(\Sigma, \tau|Y) = 0$ :

$$\operatorname{argmax}_{\Sigma, \tau} f(\Sigma, \tau|Y) = \operatorname{argmax}_{\Sigma, \tau} \frac{\ell(\Sigma, \tau|Y)}{J}.$$

The dimensions of  $\Sigma$ ,  $V$ , and  $Y$  are dependent on  $J$ , so for a particular  $J$ , we denote the corresponding  $\Sigma$  as  $\Sigma^{(J)}$ , and similarly for  $V^{(J)}$  and  $Y^{(J)}$ . Let  $a_J$  be the sequence of differences between  $\frac{\partial}{\partial \Sigma} \frac{\ell(\Sigma^{(J)}, \tau|Y^{(J)})}{J}$  and  $\frac{\partial}{\partial \Sigma} \frac{\ell(\Sigma^{(J)}, \tau|Y_{-j}^{(J)})}{J}$ :

$$a_J = \left| \frac{\partial}{\partial \Sigma} \frac{\ell(\tau, \Sigma^{(J)}|Y_{-j}^{(J)})}{J} - \frac{\partial}{\partial \Sigma} \frac{\ell(\tau, \Sigma^{(J)}|Y^{(J)})}{J} \right|.$$

If we show  $a_J \rightarrow 0$  as  $J \rightarrow \infty$ , then that is equivalent to showing  $|\operatorname{argmax}_{\Sigma} f(\Sigma, \tau|Y_{-s_j}) - \operatorname{argmax}_{\Sigma} f(\Sigma, \tau|Y)| \rightarrow 0$  as  $J \rightarrow \infty$ .

Let  $\Delta_j$  be the difference in log-likelihoods stated in Theorem B.2:

$$\begin{aligned} a_J &= \left| \frac{\partial}{\partial \Sigma} \frac{\ell(\tau, \Sigma^{(J)}|Y_{-j}^{(J)})}{J} - \frac{\partial}{\partial \Sigma} \frac{\ell(\tau, \Sigma^{(J)}|Y^{(J)})}{J} \right| \\ &= \left| \frac{\partial}{\partial \Sigma} \left( \frac{\ell(\tau, \Sigma|Y^{(J)})}{J} - \frac{\Delta_j}{J} \right) - \frac{\partial}{\partial \Sigma} \frac{\ell(\tau, \Sigma^{(J)}|Y^{(J)})}{J} \right| \\ &= \left| \frac{1}{J} \frac{\partial}{\partial \Sigma} \Delta_j \right|. \end{aligned}$$

It remains to show that  $|\frac{\partial}{\partial \Sigma} \Delta_j| \in o(J)$ . Of the terms in  $\Delta_j$ , only those involving  $V^{(J)}$  are dependent on  $J$ . The derivative is as follows:

$$\frac{\partial}{\partial \Sigma} \Delta_j = \frac{n_j/\tau^2}{1 - \frac{n_j}{\tau^2} x_j' V^{(J)} x_j} \left( \frac{1}{2} \left( 1 + \frac{\bar{e}_j^2}{1 - \frac{n_j}{\tau^2} x_j' V^{(J)} x_j} \right) \frac{\partial}{\partial \Sigma} x_j' V^{(J)} x_j + \bar{e}_j \frac{\partial}{\partial \Sigma} x_j' V^{(J)} X' Y \right).$$

Let  $a$ ,  $c$  in Lemma 3 equal  $x_j$ , then  $\frac{\partial}{\partial \Sigma} x_j' V x_j = \Sigma^{-1(J)} B V^{(J)} x_j x_j' V^{(J)} B' \Sigma^{-1(J)}$ . Let  $a = x_j$  and  $c = X' Y$ , then  $\frac{\partial}{\partial \Sigma} x_j' V X' Y = \Sigma^{-1(J)} B \tilde{\beta}^{(J)} x_j' V^{(J)} B' \Sigma^{-1(J)}$ .

From Theorem B.1, items 2 and 4, we know that  $V^{(J)}$  and  $\frac{1}{1 - \frac{n_j}{\tau^2} x_j' V^{(J)} x_j}$  decrease as  $J$  increases. We also note that  $\sqrt{n_j} \bar{e}_j = \mathcal{O}_p(\tau) \forall J$ . As the non-zero values of  $x_j$  are not dependent on  $J$ , this similarly implies that the magnitude of  $\tilde{\beta}$  is not dependent on  $J$ .

Then the partial derivatives decrease as  $J$  increases. The increase in dimension does not matter, as the solution also has  $J$  dimensions. The remaining terms are  $\mathcal{O}_p(1)$ , as we take  $\tau$  fixed. Then  $|\frac{\partial}{\partial \Sigma} \Delta_j| \in \mathcal{O}_p(1)$ .



A similar argument as above for  $\tau$  holds if  $\left| \frac{\partial}{\partial \tau} V^{(J)} \right| \in \mathcal{O}_p(1)$ . Let  $M \in \mathbb{R}^{P \times P}$  be a binary matrix where  $M_{pq} = 1$  if  $\tau^{-2}(X'X)_{pq} \neq 0$ . Then:

$$\frac{\partial}{\partial \tau} x_j' V x_j = -\frac{2}{\tau^3} x_j' V M V x_j.$$

It can be seen that this scalar quantity decreases with  $J$ , using Theorem B.1, item 1.

□

## C Table of LRR mean and standard deviation

[Table 4 about here.]

# Tables

Table 1: Comparison of assumptions and computational complexity among LCO methods for approximating  $E[Y_j|Y_{-j}]$ . Cost of Gibbs sampling for equivalent MCV problem is  $\mathcal{O}(S(N^3P + NP^2 + P^3))$ , where  $N$  = total number of data points  $Y$ ,  $P$  = number of coefficients  $\beta$ ,  $S$  = number of MC samples,  $n_j$  = size of test data for  $j^{th}$  CV fold.

Method	$f(\Sigma, \tau Y)$ vs $f(\Sigma, \tau Y_{-j})$	$f(\mu Y)$ vs $f(\mu Y_{-j})$	Bias	Time
AXE	$E[\Sigma, \tau Y] = E[\Sigma, \tau Y_{-j}]$	N/A	No	$\mathcal{O}(J(N^2P + P^3))$
GHOST	$f(\Sigma, \tau Y) = f(\Sigma, \tau Y_{-j})$	$f(\mu Y) = f(\mu Y_{-j})$	Yes	$\mathcal{O}(SJP^3)$
iIS-C	$f(\Sigma, \tau Y) \approx f(\Sigma, \tau Y_{-j})$	$f(\mu Y) \approx f(\mu Y_{-j})$	No	$\mathcal{O}(SJP^3)$
iIS-A	$f(\Sigma, \tau Y) \approx f(\Sigma, \tau Y_{-j})$	N/A	No	$\mathcal{O}(SJ(N^2P + P^3))$

Table 2: Summary of data set and model properties.  $J$  = number of CV folds,  $N$  = dimension of response vector  $Y$ ,  $n_j$  = size of test data in CV fold.

Section	Data	Model	$\Sigma$ structure	$J$	$N$	Max $n_j$
5.1	Eight schools	LMM	diagonal	8	8	1
5.2	Radon	LMM	diagonal	85	919	116
5.3	Radon subsets	LMM	diagonal	3 - 12	59 - 100	23
5.4	ESP	GLMM	diagonal	73	2160	56
5.5	SLC	GLMM	CAR	56	56	1
5.6	SRD	GLMM	CAR	271	1355	5

Table 3: Total computing time for each method and data set. Most times are provided in seconds; those marked with "h" are in hours. An asterisk (\*) indicates that a subset of 1000 MC samples was selected uniformly at random from the total of 4000 to reduce computation time; computation time in the table is an approximate obtained by multiplying actual time by 4.

Section	Data	Time				
		AXE	GHOST	iIS-C	iIS-A	MCV
5.1	Eight schools	0.3	204	539	204	557
5.2	Radon	4.0	0.6	541	56h*	1.1h
5.3	Radon subsets	1.2	90.4	3.6h	12h*	3.8h
5.4	ESP	60	0.6	720	10h*	6.1h
5.5	SLC	0.0	0.17	223	214*	0.9h
5.6	SRD	404	102h*	102h*	102h*	37.0h

Table 4: Mean and standard deviation (SD) of log RMSE ratio (LRR) for each leave-a-cluster-out CV approximation method and data set. Log RMSE ratios (LRRs), defined in Equation (7), are calculated for each CV loop. iIS-A was not applied to the SRD data due to the amount of time it would have taken.

Data	AXE		GHOST		iIS-C		iIS-A	
	Mean	SD	Mean	SD	Mean	SD	Mean	SD
Eight schools								
$\alpha < 1$	-0.05	0.45	-0.08	0.60	-0.10	0.51	-0.06	0.70
$1 \leq \alpha < 2$	-0.04	0.41	-0.15	0.58	-0.04	0.47	-0.05	0.60
$2 \leq \alpha$	0.00	0.34	-0.14	0.35	0.00	0.34	0.00	0.33
Radon								
Model 1	0.00	0.05	0.00	0.05	0.00	0.05	0.00	0.04
Model 2	-0.01	0.06	-0.02	0.07	-0.01	0.06	-0.01	0.06
Model 3	-0.01	0.03	-0.01	0.03	-0.01	0.03	0.00	0.03
Radon subsets								
Model 1	0.00	0.02	-0.03	0.03	0.00	0.02	0.10	0.10
Model 2	0.01	0.03	-0.08	0.06	0.00	0.02	0.14	0.13
Model 3	0.00	0.05	-0.18	0.20	0.00	0.05	0.23	0.21
ESP	-0.03	0.06	-0.04	0.06	1.05	0.97	0.20	0.33
SLC	0.07	0.71	0.04	0.68	0.76	1.44	0.08	0.67
SRD	-0.04	0.07	0.09	0.25	—	—	0.00	0.08

## List of Figures

- 1 Log RMSE ratios (LRRs), defined in Equation (7), are calculated for each CV loop. This figure displays box plots of the LRRs for each LCO method and data set. Horizontal bars indicate the 25%, 50%, and 75% percentiles of LRR. Vertical lines span the remainder of the data up to 1.5 times the height of the box. Points outside this span are individually annotated with dots. LRRs, defined in Equation (7), are calculated for each CV loop. In panel C, a cross ('+') is placed at -1 for those models and LCO methods with a trailing tail of large negative LRRs. . . . . 39
- 2 Scatter plots comparing the LCO approximation to ground-truth MCV estimate for each data point, model, and data set. Panels in row A compare the AXE approximation  $\hat{Y}_{ji}^{\text{AXE}}$  against the MCV estimate for  $E[Y_{ji}|Y_{-j}]$ . Panels in row B add points with GHOST (pink triangle) and iIS-C (green square) approximations, along with AXE (black circle). Each point in a grid represents one point in the corresponding data set; if multiple models were fit to the data then each point in the data set is represented once for each model. 40

# Figures

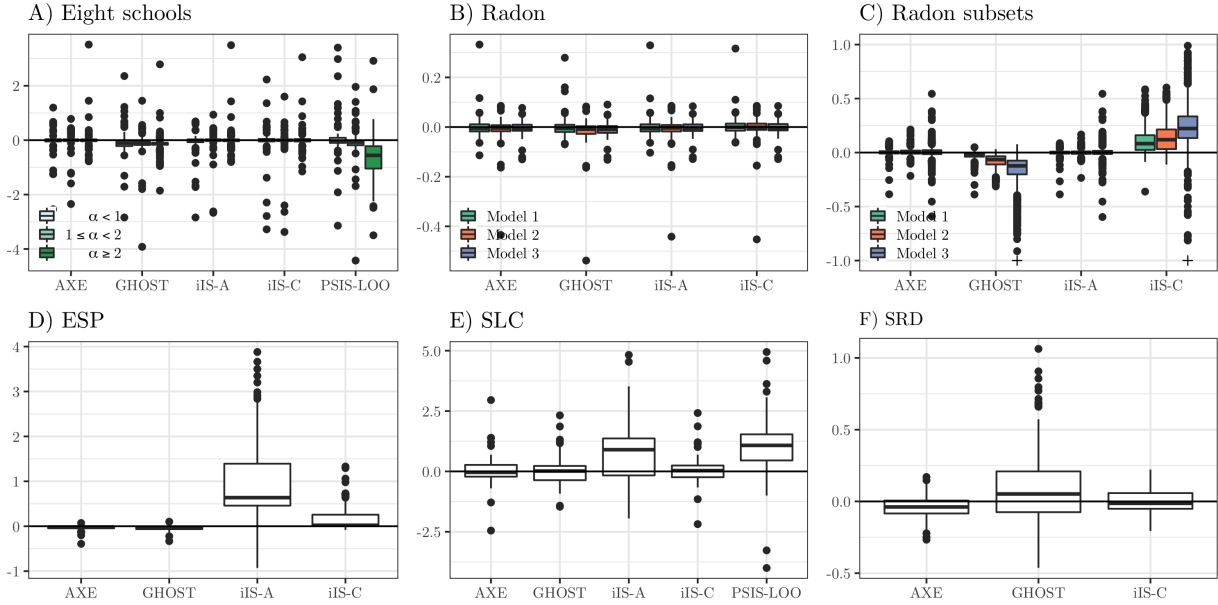


Figure 1: Log RMSE ratios (LRRs), defined in Equation (7), are calculated for each CV loop. This figure displays box plots of the LRRs for each LCO method and data set. Horizontal bars indicate the 25%, 50%, and 75% percentiles of LRR. Vertical lines span the remainder of the data up to 1.5 times the height of the box. Points outside this span are individually annotated with dots. LRRs, defined in Equation (7), are calculated for each CV loop. In panel C, a cross ('+') is placed at -1 for those models and LCO methods with a trailing tail of large negative LRRs.

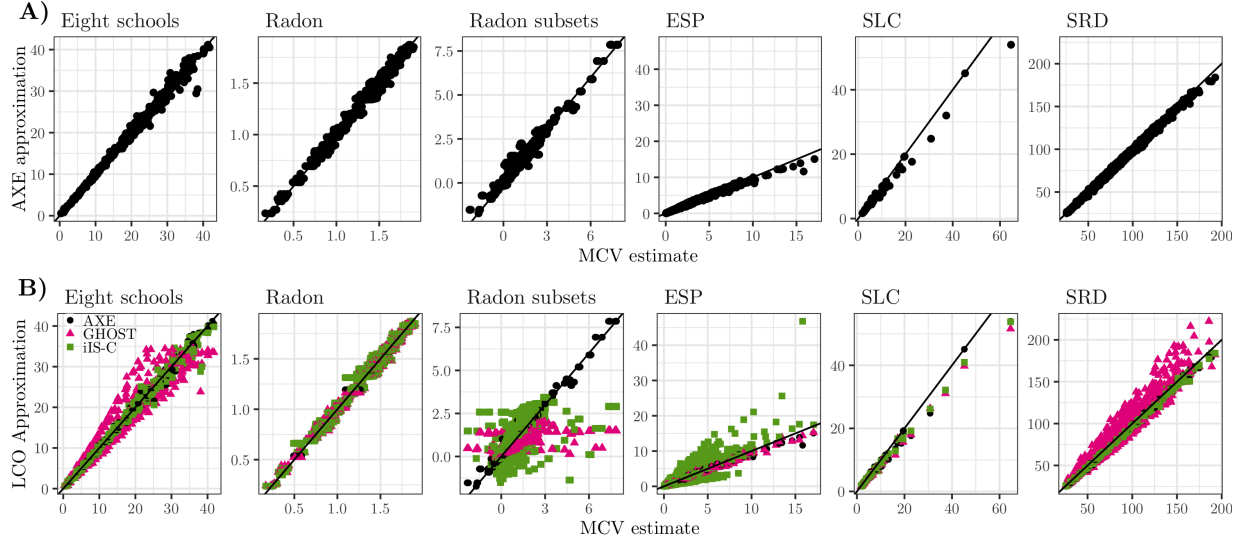


Figure 2: Scatter plots comparing the LCO approximation to ground-truth MCV estimate for each data point, model, and data set. Panels in row A compare the AXE approximation  $\hat{Y}_{ji}^{\text{AXE}}$  against the MCV estimate for  $E[Y_{ji}|Y_{-j}]$ . Panels in row B add points with GHOST (pink triangle) and iIS-C (green square) approximations, along with AXE (black circle). Each point in a grid represents one point in the corresponding data set; if multiple models were fit to the data then each point in the data set is represented once for each model.